

Dynamical quantum phase transitions and non-Markovian dynamics

Thi Ha Kyaw^{1,2,3,*}, Victor M. Bastidas,^{4,†}, Jirawat Tangpanitanon,¹, Guillermo Romero^{5,6,‡}, and Leong-Chuan Kwek^{1,7,§}

¹Centre for Quantum Technologies, National University of Singapore, 3 Science Drive 2, Singapore 117543, Singapore

²Department of Computer Science, University of Toronto, Toronto, Ontario, Canada M5S 2E4

³Department of Chemistry, University of Toronto, Toronto, Ontario, Canada M5G 1Z8

⁴NTT Basic Research Laboratories and Research Center for Theoretical Quantum Physics, 3-1 Morinosato-Wakamiya, Atsugi, Kanagawa 243-0198, Japan

⁵Departamento de Física, Universidad de Santiago de Chile, Avenida Ecuador 3493, 9170124 Santiago, Chile

⁶Center for the Development of Nanoscience and Nanotechnology, Estación Central, 9170124 Santiago, Chile

⁷MajuLab, Centre National de la Recherche Scientifique–UNS-NUS-NTU International Joint Research Unit, UMI 3654, Singapore

⁸National Institute of Education, Nanyang Technological University, 1 Nanyang Walk, Singapore 637616, Singapore



(Received 17 September 2019; revised manuscript received 4 December 2019; published 15 January 2020)

In the context of closed quantum systems, when a system prepared in its ground state undergoes a sudden quench, the resulting Loschmidt echo can exhibit zeros, resembling the Fisher zeros in the theory of classical equilibrium phase transitions. These zeros lead to nonanalytical behavior of the corresponding rate function, which is referred to as the *dynamical quantum phase transition* (DQPT). In this paper, we investigate DQPTs in the context of open quantum systems that are coupled to both Markovian and non-Markovian dephasing baths via a conserved quantity. The general framework is corroborated by studying the nonequilibrium dynamics of a transverse-field Ising ring. Our paper might shed light on theoretical developments of DQPTs in the strong system-bath coupling regime.

DOI: [10.1103/PhysRevA.101.012111](https://doi.org/10.1103/PhysRevA.101.012111)

I. INTRODUCTION

The theory of equilibrium phase transitions is well studied in statistical mechanics and thermodynamics, and it provides us with an excellent framework to understand and characterize phases of matter at zero temperature [1,2]. In the theory of classical phase transitions, nonanalytical behavior can appear in thermodynamic potentials during a phase transition. This is related to Lee-Yang zeros of the grand canonical potential [3,4] or Fisher zeros of the canonical one [5], even with a perfectly well-defined microscopic Hamiltonian without any singular interactions. To illustrate the origin of the aforementioned nonanalytical behavior, let us consider the free-energy density $f = -\lim_{N \rightarrow \infty} (N\beta)^{-1} \log[Z(\beta)]$, where N is the number of particles, β is the inverse temperature, and $Z(\beta) = \text{Tr}(e^{-\beta H})$ is the canonical partition function. From this, one can see that nonanalytical behavior in macroscopic quantities such as the free-energy density occurs whenever the partition function $Z(\beta)$ becomes zero.

In recent years, there have been many attempts to generalize the concept of Lee-Yang zeros to nonequilibrium quantum dynamics [6]. Heyl *et al.* [7] suggested that there is a dynamical counterpart of equilibrium quantum phase transitions (QPTs), referred to as dynamical quantum phase transitions (DQPTs). In fact, the concept of DQPTs is intimately related to quantum quenches in many-body systems.

Let us consider a quantum many-body Hamiltonian $\hat{H}(\lambda)$ with a quantum critical point at $\lambda = \lambda_c$. Here, λ is an external control parameter. DQPTs may be observed when a quantum system undergoes a sudden quench from $\hat{H}(\lambda_i)$ to $\hat{H}(\lambda_f)$, where λ_i and λ_f are the initial and final control parameters. Depending on the nature of the quench, there are two classes of DQPTs [8–13]. The first class, DQPT-I [14–23], describes a type of dynamical phase transition in which a time-averaged order parameter is nonzero in the long-time limit for quenches $\lambda_f < \lambda_c$, but vanishes for quenches across the critical point λ_c , i.e., $\lambda_f > \lambda_c > \lambda_i$. The second class, DQPT-II [7,24–30], generalizes the notion of nonanalyticity in the free-energy density to nonequilibrium dynamics, based on the complex Loschmidt amplitude (throughout the paper, we set $\hbar = 1$):

$$\mathcal{G}(t) = \langle \psi(0) | e^{-i\hat{H}(\lambda_f)t} | \psi(0) \rangle, \quad (1)$$

which resembles the partition function $Z(\beta)$ in statistical mechanics. Here, the initial state $|\psi(0)\rangle = |E_0(\lambda_i)\rangle$ is the ground state of the initial Hamiltonian, i.e., $\hat{H}(\lambda_i)|E_0(\lambda_i)\rangle = E_0(\lambda_i)|E_0(\lambda_i)\rangle$. Such a ground state can represent a quantum phase of matter. To investigate DQPTs, we let the system evolve under a new Hamiltonian $\hat{H}(\lambda_f)$ and study the dynamics of the return probability. The return rate associated to the Loschmidt amplitude $\mathcal{G}(t)$ is defined as

$$\zeta(t) = -\lim_{N \rightarrow \infty} \frac{1}{N} \log[\mathcal{G}(t)] \quad (2)$$

resembling the free energy in the context of classical phase transitions. In analogy to the Fisher zeros in the equilibrium statistical mechanics, one can study the zeros of the

*thihakyaw@cs.toronto.edu

†victor.bastidas@lab.ntt.co.jp

‡guillermo.romero@usach.cl

Loschmidt echo $L(t) = |\mathcal{G}(t)|^2$. The latter would lead to singular behavior of the return rate $\zeta(t)$, which has been extensively studied in the context of nonequilibrium quantum phase transitions [31–37]. In the case of the one-dimensional quantum Ising model, it has been shown that Fisher zeros of $L(t)$ form lines in the complex plane, touching the real axis only for a quench across the equilibrium critical point [7]. Thus, the zeros in $\mathcal{G}(t)$ at critical times t_c lead to nonanalyticities in $\zeta(t)$ [7,24–28,38], whenever the evolved state $|\psi(t)\rangle$ becomes orthogonal to the initial state $|\psi(0)\rangle$. Although DQPT-I and DQPT-II seem to have different origins, numerical investigations suggest that in the presence of sufficiently long-range interactions at zero temperature they are intimately related [8]. Throughout the paper, we will focus on the DQPT-II class.

Symmetry plays a fundamental role in quantum phase transitions. For example, in the thermodynamic limit, the ground state of a many-body system can exhibit less symmetries than the system Hamiltonian, a phenomenon known as spontaneous symmetry breaking. In the case of DQPT-II, we can observe a similar symmetry-breaking mechanism that can be captured by the Loschmidt amplitude. In particular, let us consider M -fold degenerate ground states $|E_0^{(j)}(\lambda_i)\rangle$ of the initial Hamiltonian $\hat{H}(\lambda_i)$, where $j = 1, \dots, M$. This degeneracy appears due to the \mathbb{Z}_M symmetry of the underlying Hamiltonian. By initializing the system in one of the ground states $|\psi(0)\rangle = |E_0^{(j)}(\lambda_i)\rangle$, one can generalize the Loschmidt amplitude by considering the probability to remain in the degenerate ground-state manifold [8,26], as follows:

$$L_{\text{Sym}}(t) = \sum_{j=1}^M |\langle E_0^{(j)}(\lambda_i) | e^{-i\hat{H}(\lambda_f)t} | \psi(0) \rangle|^2. \quad (3)$$

Here the individual terms of the sum decay exponentially with the system size N , i.e., $|\langle E_0^{(j)}(\lambda_i) | e^{-i\hat{H}(\lambda_f)t} | \psi(0) \rangle|^2 = \exp[-N(\zeta_j(t) + \zeta_j^*(t))]$. In the thermodynamic limit $N \rightarrow \infty$, only one of them dominates such that $L_{\text{Sym}}(t) = \exp[-NS(t)]$, where $S(t) = \min_j \zeta_j(t)$. In this way, the \mathbb{Z}_M symmetry, broken by the initial configuration, is restored at the critical times when all ζ_j are equal [8], leading to a cusp in $S(t)$ [25,27]. In this case, one can interpret DQPTs in terms of the dynamical restoration of symmetry [26], rather than the orthogonality between the initial state and the time-evolved state.

Strictly speaking, a nonanalyticity of the return rate occurs when the initial state becomes orthogonal to the evolved state after the sudden quench. In addition, it is not yet settled under which general circumstances such condition occurs [27,39]. However, one necessary condition seems to be the existence of a sufficiently strong quench, which is achieved when a system parameter λ is quenched across an underlying equilibrium critical point λ_c . Recent experiments in trapped ions [22,27], ultracold atoms in optical lattices [40], and quantum simulation by using superconducting qubits [41] seem to support this feature. Nevertheless, it is also interesting to note that there is no one-to-one correspondence between DQPTs and equilibrium QPTs. It is possible to have nonanalytical behavior in the return rate without crossing an equilibrium critical point λ_c in the quench, and one can cross a critical

point during a quench without divergencies in the return rate [42]. In addition, there is a recent attempt to relate DQPTs and equilibrium QPTs near the vicinity of a DQPT in the transverse-field Ising chain [43].

In general, when a quantum system is in a statistical ensemble, it is convenient to use the density-matrix formalism. Therefore, in order to extend the notion of DQPTs to mixed states, a generalization of the Loschmidt amplitude Eq. (1) in terms of density matrices is indispensable. There are two ways to achieve this. First, there is *the interferometric Loschmidt amplitude* [12,39,44]

$$\mathcal{G}_I(t) = \text{Tr}[\hat{\rho}(0)\hat{U}(t, 0)], \quad (4)$$

which is a direct extension of Eq. (1), where $\hat{\rho}(0)$ is the density matrix at initial time and $\hat{U}(t, 0)$ is the unitary evolution operator from the initial time to later time t . This method is useful when a system, initially prepared in a statistical ensemble, undergoes a unitary evolution via a sudden quench without interacting with an external environment. However, the interferometric Loschmidt amplitude $\mathcal{G}_I(t)$ cannot be used when the dynamics are nonunitary, i.e., when the system couples to a reservoir. Second, there is *the fidelity Loschmidt amplitude* defined as

$$\mathcal{G}_F(t) = \text{Tr}[\sqrt{\sqrt{\hat{\rho}(0)}\hat{\rho}(t)\sqrt{\hat{\rho}(0)}}], \quad (5)$$

which is a metric, measuring the distance between the time-evolved density matrix $\hat{\rho}(t)$ and the initial one $\hat{\rho}(0)$. Furthermore, the fidelity Loschmidt amplitude [12,45–47] and related measures [48] have proven useful for analyzing DQPT-II when including dissipative mechanisms. The advantage of this formulation is that $\hat{\rho}(t)$ can now evolve under both unitary and nonunitary dynamics. In the present paper, we adopt the latter quantifier.

In this paper, our goal is to understand how dephasing channels acting upon quantum systems affect the fidelity Loschmidt amplitude and signatures of DQPTs. In particular, we consider quenches in the context of open quantum systems that are described by Lindblad-type master equations. Furthermore, we investigate the effect of non-Markovian environment [49] on DQPT signatures experienced by a quantum Ising spin chain. To the best of our knowledge, there are no previous works describing the effect of a non-Markovian environment on DQPTs. Based on an open quantum system approach, we obtain an exact master equation that is valid for any coupling strength between the spin chain and the dephasing bath.

This paper is organized as follows. First, we introduce a physical model we study in Sec. II. Then, we discuss a general framework to describe a system coupled to both Markovian and non-Markovian baths in Sec. III. We then apply the general framework to a paradigmatic model: a one-dimensional transverse Ising model with periodic boundary conditions. In addition, we discuss signatures of DQPTs of the Ising chain under Markovian and non-Markovian dynamical evolutions in Sec. IV. In Sec. V, we show non-Markovian DQPTs under continuous bath degrees of freedom. Lastly, we provide concluding remarks and an outlook in Sec. VI.

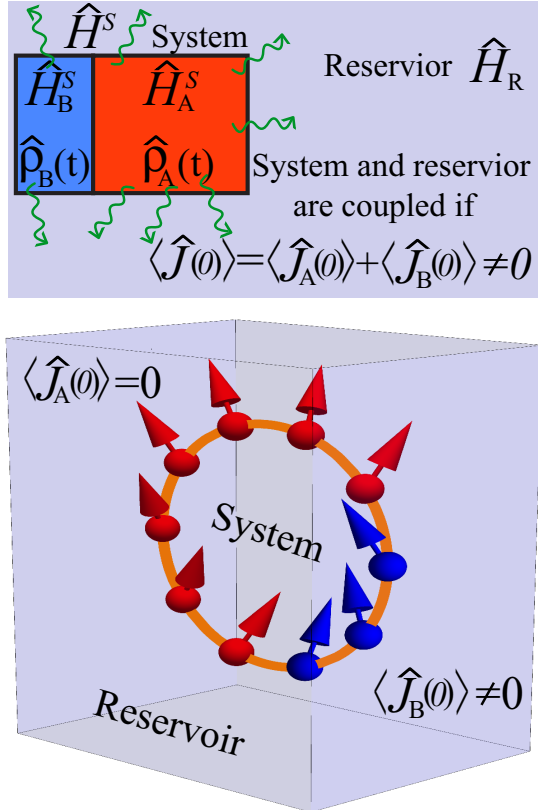


FIG. 1. Open quantum system approach to DQPTs. The system of interest with Hamiltonian \hat{H}^S is composed of two transverse Ising chains A and B depicted in red and blue, respectively. The spin chain A is initialized in one of the ground states of the Hamiltonian \hat{H}_A^S without current $\langle \hat{J}_A(0) \rangle = 0$, while the spin chain B is initialized in a ground state of the Hamiltonian \hat{H}_B^S , which plays the role of an energy current source $\langle \hat{J}_B(0) \rangle \neq 0$. The entire ring is coupled to the environment via a conserved quantity \hat{J} which is the total energy current. The system \hat{H}^S is coupled to the environment \hat{H}_R when the initial total current is different from zero, i.e., $\langle \hat{J}(0) \rangle = \langle \hat{J}_A(0) \rangle + \langle \hat{J}_B(0) \rangle \neq 0$.

II. THE SETUP

The system we consider is the Ising ring composed of two transverse Ising chains A and B as seen in Fig. 1. The Ising ring Hamiltonian is

$$\hat{H}^S = -\tau \sum_{j=1}^{N-1} \hat{\sigma}_j^x \hat{\sigma}_{j+1}^x - h \sum_{j=1}^N \hat{\sigma}_j^z, \quad (6)$$

where $\hat{\sigma}^{z/x}$ are the Pauli matrices and $N = N_A + N_B$ is the sum of the total spins from the two subsystems. In the following, the sites $j = 1, \dots, N_A$ label the Ising chain A and $j = N_A + 1, \dots, N$ label the Ising chain B . The Hamiltonian (6) has been extensively studied [1] and can be solved analytically even for its sudden quench dynamics in certain limits (see Ref. [2] and references therein). The transverse Ising model has a quantum critical point $\tau = h$ [1] at 0-K temperature. Furthermore, if the Ising chain is put into a ring geometry with the periodic boundary condition, $\hat{\sigma}_{N+1} = \hat{\sigma}_1$, as shown in Fig. 1, a conserved quantity known as the global current \hat{J}

naturally arises [50,51], i.e., $[\hat{H}^S, \hat{J}] = 0$ (see Appendix A for its derivation). The expression for the conserved current, the Dzyaloshinskii-Moriya (DM) interaction, is

$$\hat{J} = \frac{\hbar\tau}{2} \sum_j \hat{\sigma}_j^y (\hat{\sigma}_{j-1}^x - \hat{\sigma}_{j+1}^x). \quad (7)$$

One can define local currents \hat{J}_A and \hat{J}_B for the Ising chains A and B , respectively. In contrast to the global current \hat{J} , the local currents are not conserved quantities. One can obtain its explicit expressions by using Eq. (7) with $j = 1, \dots, N_A$ for the Ising chain A and $j = N_A + 1, \dots, N$ for the Ising chain B . In this paper, we will treat the Ising chain A as a current drain and B as a current source, which will be clarified below.

As we have mentioned earlier, DQPT is observed when a quantum system undergoes a sudden quench across the equilibrium critical point, and signatures of DQPT can be captured via the minimization principle [26,27]. Here, we use this minimization procedure within the open quantum systems framework of Floquet stroboscopic divisibility that we proposed in a recent work [49] (see Appendix B). In particular, we consider a particular quench protocol, which involves three steps. First, we initialize the Ising chain A in one of the degenerate ground states of $\hat{H}_A^S = -\tau \sum_{j=1}^{N_A-1} \hat{\sigma}_j^x \hat{\sigma}_{j+1}^x$, since it has broken \mathbb{Z}_2 symmetry. In particular, $|\psi_+\rangle = |\rightarrow\rightarrow\dots\rightarrow\rangle$ and $|\psi_-\rangle = |\leftarrow\leftarrow\dots\leftarrow\rangle$, where $\sigma_i^x |\psi_\pm\rangle = \pm |\psi_\pm\rangle, \forall i \in A$. We take $|\psi_+\rangle$ as the initial state for the chain A . Second, we take the chain B initial state as the ground state $|\psi_G\rangle$ of the following Hamiltonian:

$$\hat{H}_B^S = -\tau \sum_{j=N_A+1}^{N-1} \hat{\sigma}_j^x \hat{\sigma}_{j+1}^x - h \sum_{j=N_A+1}^N \hat{\sigma}_j^z - v \hat{J}_B. \quad (8)$$

Here, the expression of \hat{J}_B differs from the global current operator since it only applies to the chain B with open boundary condition. Its boundary terms consist of $-\hat{\sigma}_{N_A+1}^y \hat{\sigma}_{N_A+2}^x$ and $\hat{\sigma}_N^y \hat{\sigma}_{N-1}^x$. The parameter v controls the amount of energy current present inside the ring. In this way, we induce the energy current inside the chain B [50]. By combining the Ising chains A and B , one forms an Ising ring with a conserved energy current \hat{J} throughout its evolution, obtained from $|\psi_G\rangle_B$. Hence, we refer to the subsystem A as “drain” and the subsystem B as “source.” Now we can define the initial state of the Ising ring as $|\psi(0)\rangle = |\psi_+\rangle_A \otimes |\psi_G\rangle_B$, from which we construct the initial density matrix of the system $\hat{\rho}_S(0) = |\psi_+\rangle \langle \psi_+|_A \otimes |\psi_G\rangle \langle \psi_G|_B$.

III. DQPTS IN AN OPEN QUANTUM SYSTEM

To derive the exact master equation with the Floquet stroboscopic divisibility [49], in this paper, we are looking at a specific model, where the Ising ring couples to external baths via the global energy current \hat{J} , as shown in Fig. 2. We also consider an uncorrelated initial state $\hat{\rho}(0) = \hat{\rho}_S(0) \otimes \hat{\rho}_R(0)$, where $\hat{\rho}_S(0)$ and $\hat{\rho}_R(0)$ are the initial states of the system and reservoir, respectively. We quench the entire chain with the Hamiltonian of the total system (see Table I for the quench protocol):

$$\hat{H} = \hat{H}^S + \hat{J} \sum_l \hat{X}^l + \hat{H}_R. \quad (9)$$

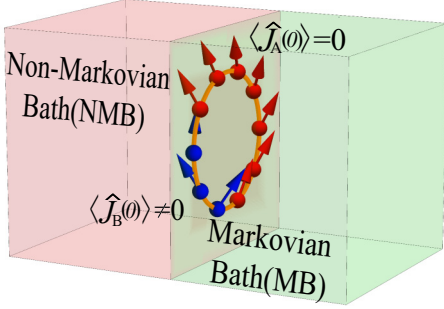


FIG. 2. The Ising spin ring, in Fig. 1, is globally coupled with both Markovian and non-Markovian dephasing baths. The bath degrees of freedom are captured via quantum bosonic modes. The two baths do not interact each other.

In this expression, the global coupling between the Ising ring and the reservoir is defined in terms of the operator $\hat{X}^l = \hat{X}_{\text{MB}}^l + \hat{X}_{\text{NMB}}^l$, where $\hat{X}_{\text{NMB}}^l = g_l(\hat{b}_l^\dagger + \hat{b}_l)$ and $\hat{X}_{\text{MB}}^l = \tilde{g}_l(\hat{c}_l^\dagger + \hat{c}_l)$ are the quadratures of the non-Markovian (NMB) and Markovian (MB) baths, respectively. Similarly, $\hat{H}_R = \hat{H}_{\text{MB}} + \hat{H}_{\text{NMB}}$ is the Hamiltonian of the reservoir, where $\hat{H}_{\text{MB}} = \sum_l \tilde{\omega}_l \hat{c}_l^\dagger \hat{c}_l$ and $\hat{H}_{\text{NMB}} = \sum_l \omega_l \hat{b}_l^\dagger \hat{b}_l$. Note that the coupling to the dephasing baths is via a current operator \hat{J} resembling the DM interaction in spin systems [52,53]. In this paper, we consider the non-Markovian coupling strength $g_l = (\eta/\Omega^2)e^{-z_l/2}$, where $z > 0$ is a positive number, and the modes of the non-Markovian bath have frequencies $\omega_l = l\Omega$ ($l = 1, 2, \dots, M$), where Ω is the fundamental frequency. Notice that the choice of units for g_l is consistent with units of the energy current \hat{J} , so that the Ising ring-bath coupling has frequency in units such that $\hbar = 1$.

According to the above description, the Ising ring evolves under the Lindblad-type master equation $d\hat{\rho}_S(t)/dt = -i[\hat{H}^S(t), \hat{\rho}_S(t)] + \gamma(t)\hat{D}[\hat{J}]\hat{\rho}_S(t)$, where $\hat{D}[\hat{J}]\hat{\rho}_S(t) = \hat{J}\hat{\rho}_S(t)\hat{J} - \frac{1}{2}(\hat{J}^2\hat{\rho}_S(t) + \hat{\rho}_S(t)\hat{J}^2)$ and $\hat{H}^S(t) = \hat{H}^S - \lambda(t)\hat{J}^2$, where there is a Lamb shift term proportional to

$$\lambda(t) = \sum_{l=1}^M \frac{g_l^2}{\omega_l} [1 - \cos(\omega_l t)]. \quad (10)$$

Also, the dephasing rate reads

$$\gamma(t) = 2\gamma_0 + 2\gamma_1(t), \quad (11)$$

where γ_0 and $\gamma_1(t) = \sum_{l=1}^M \frac{g_l^2}{\omega_l} \sin(\omega_l t) \coth(\beta_{\text{NMB}}\omega_l/2)$ are the dephasing rates associated with the Markovian and non-Markovian baths, respectively. Due to the choice of the frequencies of the bath $\omega_l = l\Omega$, the functions $\lambda(t)$ and $\gamma(t)$ are periodic with a period $T = 2\pi/\Omega$. We also consider that the non-Markovian is initially prepared in a thermal state with

inverse temperature β_{NMB} . Note that in the previous equations M denotes the number of modes of the non-Markovian bath. It is worth mentioning that a crucial point in obtaining the above Lindblad equation is that both baths couple to a conserved quantity of the system, in our case, $[\hat{H}^S, \hat{J}] = 0$. Thus, the theory we consider may apply to any quantum system experiencing DQPT that couple to dephasing baths via global or local conserved quantities. See Appendix B and Ref. [49] for a detailed explanation of the open quantum system theory. One important aspect of the master equation is that due to the time-periodic character of the rates the dynamics of the Ising ring is divisible at stroboscopic times, which is referred to as Floquet stroboscopic divisibility [49].

So far, we have derived the exact master equation governing the evolution of the Ising ring. In this paper, we focus on signatures of DQPTs that appear in the dynamics of the spin chain A, described by the reduced density matrix $\hat{\rho}_A(t) = \text{Tr}_B[\hat{\rho}_S(t)]$. During the quench, the indirect signatures of the DQPTs for a finite system size [27] can be obtained by measuring the two probabilities [26] to return to the same initial ground state or the other [see Eq. (5)], $\mathcal{G}_{F,d} = \text{Tr}[\sqrt{\hat{\rho}_d}\hat{\rho}_A(t)\sqrt{\hat{\rho}_d}]$, where $d \in \{+, -\}$, $\hat{\rho}_+ = |\psi_+\rangle\langle\psi_+|$, and $\hat{\rho}_- = |\psi_-\rangle\langle\psi_-|$. Hence, the time-dependent rate function becomes

$$\varpi(t) \equiv \min_{d \in \{+, -\}} \{-N^{-1} \log[\mathcal{G}_{F,d}(t)]\}. \quad (12)$$

In order to characterize signatures of DQPTs within the framework of Floquet stroboscopic divisibility, we consider the initial state of the Ising chain A as one of the broken \mathbb{Z}_2 symmetry states of $\hat{H}_A^{S_1}$, while the current source is generated by the ground state of $\hat{H}_B^{S_1} + \hat{H}_B^{S_2} - \nu\hat{J}_B$, where $\hat{H}_B^{S_2} = -h \sum_{j=N_A+1}^N \hat{\sigma}_j^z$. During the quench, both of the subsystems would interact with the environment via the system-bath coupler $\hat{J} \sum_l \hat{X}^l$.

If there is no current present inside the Ising ring, the dephasing channel plays no role, independent of how strongly the system couples to the baths. The system is coupled to the environment when the initial total current is nonzero, i.e., $\langle \hat{J}(0) \rangle = \langle \hat{J}_A(0) \rangle + \langle \hat{J}_B(0) \rangle \neq 0$. For simplicity, let us consider the Ising ring coupled to a Markovian bath. Numerical evidence from Fig. 3, where we plot the return rate function ϖ for three different decay rates γ_0 , clearly supports our discussion. To overcome this, we introduce the current $\langle \hat{J}_B(0) \rangle \neq 0$ inside the subsystem B at the start of the quench.

Furthermore, our open quantum system approach (see Appendix B) allows us to tune the system-bath interactions to study different scenarios involving (i) only a Markovian bath, (ii) only a non-Markovian bath, (iii) the combined effects of both Markovian and non-Markovian baths, by changing the values of γ_0 and γ_1 (see Fig. 4). In this way, we can study the

TABLE I. State preparation protocol before the quench, followed by the quench protocol, with which our quantum system evolves under the influence of the Markovian and non-Markovian bath.

Quench	Subsystem A	Subsystem B	Bath	System bath coupling
Before, prepared in	One of the ground states of $\hat{H}_A^{S_1}$	Ground state of $\hat{H}_B^{S_1} + \hat{H}_B^{S_2} - \nu\hat{J}_B$		
During, evolved under	$\hat{H}_A^{S_1} + \hat{H}_A^{S_2}$	$\hat{H}_B^{S_1} + \hat{H}_B^{S_2}$	\hat{H}_R	$\hat{J} \sum_l \hat{X}^l$

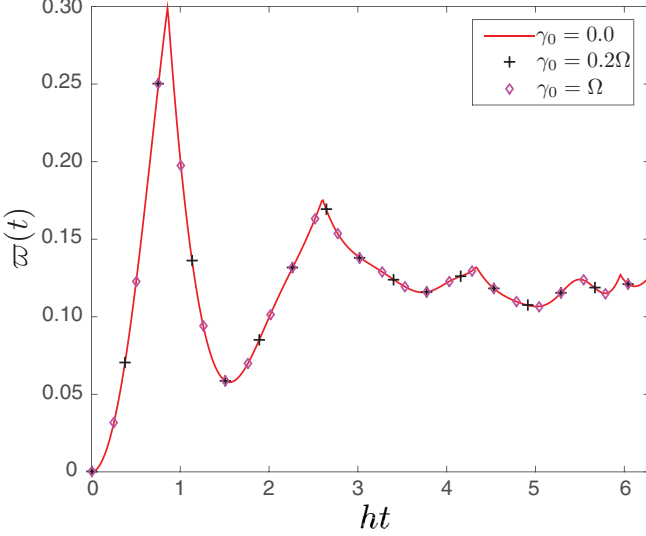


FIG. 3. Time-dependent rate function in one period T plotted for various decay rates associated with different Markovian baths. We have $N_A = 6$ spins for the subsystem A and $N_B = 2$ spins for the subsystem B . The interspin coupling is $\tau = 0.42\Omega$ and the transverse magnetic field $h = \Omega$. There is no current present in the subsystem B initially, i.e., $v = 0$ in Eq. (8). Thus, the entire ring does not couple to the environments as seen in a single return rate for three different Markovian decay rates.

effect of system-bath coupling on the signatures of DQPTs. The rate $\gamma_1(t)$ is a periodic function, the average of which is zero in one period, as seen in Fig. 4(a). The dephasing rate γ_0 controls the overall sign of the dephasing rate $\gamma(t)$, since it acts like a dc signal. By tuning the dephasing rate γ_0 one can control if the dynamics is Markovian [$\gamma(t) \geq 0$ for all times $t > 0$] or non-Markovian when the rate becomes negative at certain time intervals. The time-dependent dephasing rate is

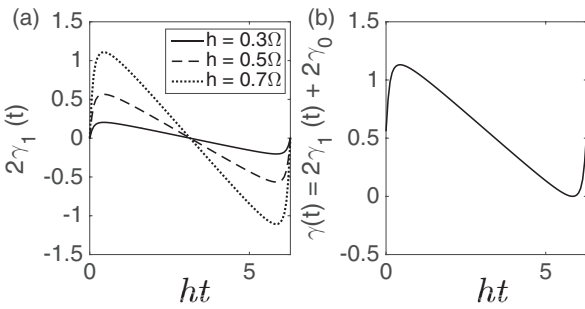


FIG. 4. (a) Various $\gamma_1(t)$ vs time ($1T$) plotted for three different values of $h = 0.3\Omega, 0.5\Omega, 0.7\Omega$. As seen from the figure, γ_1 exhibits both positive and negative values, with which the negative ones will contribute towards non-Markovian dynamics [49]. From the plots, we obtain the maximum values that are then used for Markovian dephasing rates in the upcoming numerical analyses. (b) Total $\gamma(t)$ plotted in $1T$ for $\gamma_0 = \max[\gamma_1(t)] = 0.2827\Omega$, and $\eta = 0.5\Omega$, such that the entire $\gamma(t)$ does not have negative value within one period. Hence, we are in complete Markovian evolution. We consider $M = 60$ bosonic modes in the non-Markovian bath. See Appendix B for the open quantum system framework used.

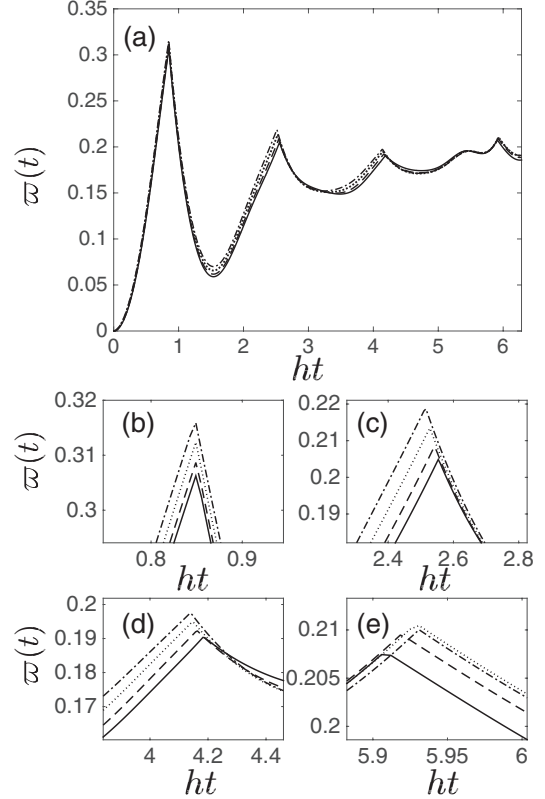


FIG. 5. (a) Time-dependent rate function in one period T plotted for various decay rates associated with different Markovian decay rates γ_0 . Solid line, $\gamma_0 = 0$; dashed line, $\gamma_0 = 0.1018\Omega$; dotted line, $\gamma_0 = 0.2827\Omega$; dot-dashed line, $\gamma_0 = 0.5542\Omega$. (b)–(e) Enlarged regions of four different critical times seen in (a). We have $N_A = 6$ spins for the subsystem A and $N_B = 2$ spins for the subsystem B . The interspin coupling is $\tau = 0.42\Omega$, the transverse magnetic field $h = \Omega$, and $v = 5\Omega$. $\eta = 0$ for all the plots and $z = 0.1$. The number of bosonic modes in the non-Markovian bath is $M = 60$.

depicted in Fig. 4(b). In all our numerical calculations we set the parameters in terms of the fundamental frequency Ω that defines the period $T = 2\pi/\Omega$ of the dephasing rate $\gamma(t+T) = \gamma(t)$. For a more detailed discussion of non-Markovian dynamics in master equations with time-periodic rates, we refer the reader to Ref. [49].

In Fig. 5, we show numerical evidence of the DQPTs for various Markovian dephasing rates, in terms of the time-dependent rate function $\bar{\gamma}(t)$. We show the enlarged regions of the four particular critical times seen in Fig. 5(a) in the order of appearance in Figs. 5(b)–5(e). It is evident that when the dephasing rate increases we see the shift in the dynamical critical times towards the left as compared to the closed system case (the black solid line), in particular (c) and (d). In the case of non-Markovian dynamics, we consider $\gamma(t) = \gamma_1(t)$ and choose the coupling parameter h in such a way that its maximum value $\max[\gamma(t)] = \gamma_0$ will correspond to γ_0 used in Fig. 5. In Figs. 5 and 6, the critical times shift towards the left for the second and third peaks. However, we observe the right shift at the last peak with the increase in the system-bath coupling strengths.

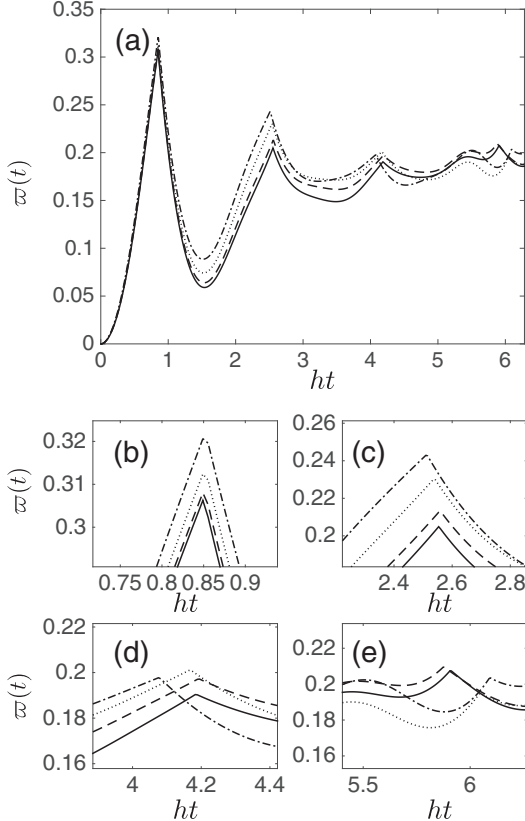


FIG. 6. (a) Time-dependent rate function in one period T plotted for various decay rates associated with different coupling strengths to the non-Markovian bath: $\eta = 0$, solid line; $\eta = 0.3\Omega$, dashed line; $\eta = 0.5\Omega$, dotted line; $\eta = 0.7\Omega$, dot-dashed line. (b)–(e) Enlarged regions of four different critical times seen in (a). We choose the decay rates such that $\max[\gamma(t)] = \gamma_0$, where γ_0 are the parameters used in Fig. 5. We have $N_A = 6$ spins for the subsystem A and $N_B = 2$ spins for the subsystem B . The interspin coupling is $\tau = 0.42\Omega$, the transverse magnetic field $h = \Omega$, and $v = 5\Omega$. We choose a dephasing rate $\gamma(t) = \gamma_1(t)$ for all the plots and $z = 0.1$ and the number of bosonic modes in the non-Markovian bath is $M = 60$.

IV. INTERPLAY BETWEEN NON-MARKOVIAN AND MARKOVIAN ENVIRONMENTS

In Figs. 5 and 6, effects of both Markovian and non-Markovian baths on the DQPTs signatures are not obvious when we look at the rate function $\varpi(t)$. However, the difference between both baths is clear if we consider an order parameter such as the average magnetization $M_x = \langle \sum_j \hat{\sigma}_x^j \rangle$ (see Fig. 7). Here, shifts in singularities of the rate function are not pronounced for different system-bath coupling strengths in both Markovian and non-Markovian dynamics. On the other hand, we observe the usual oscillatory decay of the average magnetization in both cases. However, the oscillations are more pronounced in the non-Markovian cases, even at time scales where the oscillations disappear under the effect of a Markovian bath. During the non-Markovian evolution, the increase in oscillation frequency of the order parameter is observed with increase in the system-bath coupling strength as indicated by the green dotted line. The reason is that the

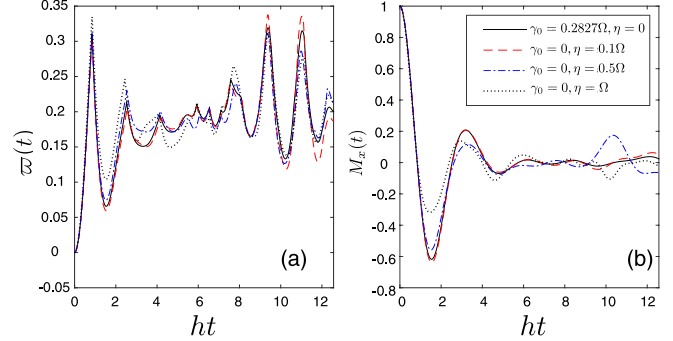


FIG. 7. (a) Time-dependent rate function and (b) the average magnetization in two periods ($2T$) plotted for purely Markovian dynamics (black solid line) and non-Markovian ones (the rest, with different system-bath coupling strengths). We observe shifts in singularities of the rate function, but this behavior is not pronounced for different system-bath coupling strengths. The usual oscillatory decay of the order parameter M_x is present for both cases, but nonzero oscillations are present in non-Markovian evolution while a near-zeroth-order parameter is observed in the Markovian dynamics. In this simulation we have used the same interspin coupling, transverse magnetic field, and number of bosonic modes as in Fig. 6.

bath influences the system dynamics as a form of feedback excitation [49].

V. BOSONIC BATH IN THE CONTINUUM LIMIT

So far, we have discussed the open quantum system evolution with finite bosonic bath degrees of freedom. However, we can take the bath degrees of freedom to the continuum limit. Consider an Ohmic spectral bath density:

$$J(\omega) = \frac{\omega^s}{\omega_c^{s-1}} e^{-\omega/\omega_c}, \quad (13)$$

where ω_c is the cutoff frequency and s is the Ohmicity parameter. With it, we can recalculate $\Gamma(t)$ as

$$\Gamma(t) = 4 \int d\omega J(\omega) \frac{1 - \cos(\omega t)}{\omega^2}, \quad (14)$$

from which we can find out the dephasing rate $\gamma(t)/2 = \dot{\Gamma}(t)$. The Ohmicity parameter $s > 2$ [54] gives rise to a nonzero value for all non-Markovianity measures [55–57]. In Fig. 8, we show the return rate function in one period evolution time where we change the Ohmicity parameter from $s = 1$ to 5, starting from purely Markovian dynamics and transitioning to the non-Markovian regimes. We see shifts in the critical times for various s . The results are similar to what we observed previously and the DQPT signatures are not much affected by the types of environment the system interacts with. However, when we look at the average magnetization over different s 's, we see the pronounced oscillations as we cross over to the non-Markovian regime. Here, we have a single type of bath (Markovian or non-Markovian) at all times. The treatment is different from previous sections where we rely on the Floquet stroboscopic divisibility [49] to reach non-Markovian dynamics.

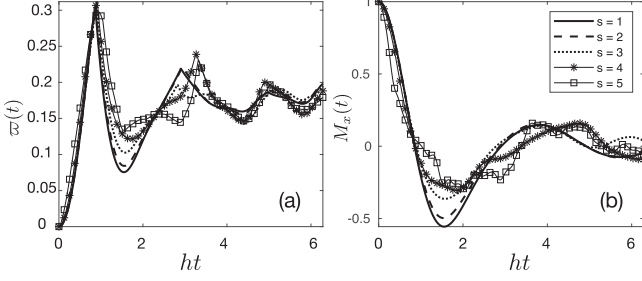


FIG. 8. (a) Time-dependent rate function in one period T and (b) average magnetization plotted for various Ohmicity parameters s . In these simulations, we have used the same interspin coupling and transverse magnetic field as in Fig. 6. We note that the simulations here are different from the previous results in that there is no change of system-bath coupling. We only change the parameter s for the continuum of bosonic modes. Here, we have $v = 1$, $h = \omega_c$, $\tau = 0.42\omega_c$.

VI. DISCUSSIONS AND OUTLOOK

We have presented a theoretical framework to investigate dynamical quantum phase transitions under the action of Markovian and non-Markovian dephasing baths. We have shown that with the help of the Floquet stroboscopic dynamics one can tune the Markovian and non-Markovian dynamics to observe their effects on the DQPTs signatures. In particular, we have studied the paradigmatic transverse field Ising model with periodic boundary condition. There, the energy current is a conserved quantity, which we use to couple the Ising ring to Markovian and non-Markovian dephasing baths. We show that indirect measurements of DQPT using the minimization principle discussed in Ref. [27] do not distinguish between Markovian and non-Markovian dynamics, even though the average magnetization differentiates the two. Furthermore, we show there are two ways to change the physical system to undergo non-Markovian dynamics. One is to change the current flow inside the ring while keeping the system-bath coupling constant, i.e., to increase or decrease the value of v in \hat{H}_B^S . Another way is to change the system-bath coupling η keeping the current v constant. Lastly, we also present that our master equation approach to non-Markovian dynamics can be extended to continuous Ohmic spectral bath density. By adjusting the Ohmicity parameter, we can tune the underlying dynamics to be Markovian or non-Markovian. To sum up, we have studied a very specific open quantum system: a dephasing model for the DQPTs under Markovian and non-Markovian dynamics. We have used an indirect method to deduce the DQPT signatures using the minimization principle. The indifference results in Markovian and non-Markovian dynamics suggest an inability to distinguish the two open system dynamics by the minimization principle. We believe our paper can open up a new window of opportunities in the direction of nonequilibrium quantum phase transitions with strong system-bath coupling.

ACKNOWLEDGMENTS

Fruitful discussion with Jad Halimeh is acknowledged. The authors are grateful for financial support through the National

Research Foundation and the Ministry of Education Singapore. G.R. acknowledges support from the Fondo Nacional de Desarrollo Científico y Tecnológico (FONDECYT, Chile) under Grant No. 1190727.

APPENDIX A: DERIVATION OF THE CONSERVED QUANTITY: THE GLOBAL CURRENT

A general flux (current) operator may be obtained by assuming that there exists an operator continuity equation in one dimension [51]:

$$\frac{\partial \hat{h}(x, t)}{\partial t} + \frac{\partial \hat{j}(x, t)}{\partial x} = 0, \quad (\text{A1})$$

where $\hat{h}(x, t)$ and $\hat{j}(x, t)$ are the energy density and the energy flux operators, respectively. For an N -site chain with m states at each site, one can write down the energy density operator as

$$\hat{h}(x, t) = \sum_s \hat{h}_s \delta(x - x_s), \quad (\text{A2})$$

with \hat{h}_s being the discrete energy operator at the site s and $\delta(x - x_s)$ being the Dirac delta function, so that the system Hamiltonian reads $\hat{H} = \int dx \hat{h}(x, t) = \sum_s \hat{h}_s$. Similarly, the energy flux operator is

$$\hat{j}(x, t) = \sum_s \hat{j}_s \delta(x - x_s), \quad (\text{A3})$$

where \hat{j}_s is the current operator at the s th site. Under these definitions, the continuity equation adopts the following discrete form:

$$\frac{\partial \hat{h}(x, t)}{\partial t} = \sum_s \frac{d\hat{h}_s}{dt} \delta(x - x_s), \quad (\text{A4})$$

$$\frac{\partial \hat{j}(x, t)}{\partial x} = \sum_s -\left(\frac{\hat{j}_{s-1} - \hat{j}_s}{a}\right) \delta(x - x_s), \quad (\text{A5})$$

$$\frac{d\hat{h}_s}{dt} = \frac{\hat{j}_{s-1} - \hat{j}_s}{a}, \quad (\text{A6})$$

where a is the spacing between any $j+1$ th and j th sites. The time evolution of the operator \hat{h}_s in the Heisenberg picture reads

$$\frac{d\hat{h}_s}{dt} = i[\hat{H}, \hat{h}_s]. \quad (\text{A7})$$

To proceed further, one may consider a generic one-dimensional Hamiltonian with up to two-body nearest-neighbor interactions:

$$\hat{H} = \sum_s [\hat{h}_s^0 + \hat{V}(s, s+1)], \quad (\text{A8})$$

where \hat{h}_s^0 is the local Hamiltonian at site s , and $\hat{V}(s, s+1)$ are the site-dependent two-body interaction terms. When we invoke this discretization formalism to the Ising ring model (see Fig. 1), we arrive at the global current operator [50]:

$$\hat{j} = \frac{H\tau}{2} \sum_j \hat{\sigma}_j^y (\hat{\sigma}_{j-1}^x - \hat{\sigma}_{j+1}^x). \quad (\text{A9})$$

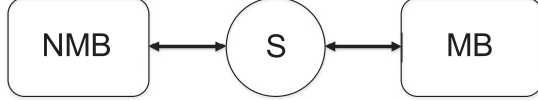


FIG. 9. An arbitrary quantum system (S) interacts with both Markovian and non-Markovian baths labeled as “MB” and “NMB” respectively.

We note that the terms inside the above summation comprise the Dzyaloshinskii-Moriya interaction in the theory of weak ferromagnetism [52,53]. One direct consequence is that we have a conserved quantity \hat{J} such that $[\hat{H}^S, \hat{J}] = 0$ when we have a closed boundary condition, i.e., $\hat{\sigma}_{N+1} = \hat{\sigma}_1$.

APPENDIX B: A ROADMAP TO NON-MARKOVIAN OPEN QUANTUM SYSTEMS

Let us denote a system Hamiltonian as \hat{H}_S , where it can, in principle, be a quantum Ising chain, atom-atom interaction in ultracold atoms lattices, Bose-Hubbard model, etc. The environment degrees of freedom are captured by bosonic harmonic oscillators. We denote it as \hat{H}_R , which is composed of $\hat{H}_{\text{NMB}} = \sum_j \omega_j \hat{b}_j^\dagger \hat{b}_j$ and $\hat{H}_{\text{MB}} = \sum_j \tilde{\omega}_j \hat{c}_j^\dagger \hat{c}_j$. $\hat{b}(\hat{b}^\dagger)$ are bosonic annihilation (creation) operators for the non-Markovian bath, while $\hat{c}(\hat{c}^\dagger)$ are bosonic annihilation (creation) operators for the Markovian one. The setup is that the system described by \hat{H}_S couples globally to the environment \hat{H}_B via a conserved quantity as depicted in Fig. 9. A microscopic derivation of the reduced system dynamics is obtained by considering the following total Hamiltonian:

$$\hat{H} = \hat{H}_S + \hat{V}_S \sum_l \hat{X}^l + \hat{H}_R, \quad (\text{B1})$$

where \hat{V}_S is the system operator and $\hat{X}^l = \hat{X}_{\text{MB}}^l + \hat{X}_{\text{NMB}}^l$. For simplicity, we choose \hat{X}_{NMB}^l and \hat{X}_{MB}^l to be of the form $\kappa_l(\hat{\Theta}_l^\dagger + \hat{\Theta}_l)$. We remark that $\kappa_l = g_l$ represents the coupling between the system operator and the bosonic mode ω_j of the non-Markovian ($\hat{\Theta} = \hat{b}$) and $\kappa_l = \tilde{g}_l$ is the Markovian coupling with $\tilde{\omega}_l$ bosonic modes ($\hat{\Theta} = \hat{c}$). M is the total number of modes inside each reservoir. Although the system-bath coupling is treated globally, it is noteworthy that our previous work [49] also applies to the local system-bath coupling. The only constraint we impose to derive our microscopic master equation reads

$$[\hat{H}_S, \hat{V}_S] = 0. \quad (\text{B2})$$

Whenever the above constraint, Eq. (B2), is satisfied, we can always find the reduced density matrix of the system analytically [49], and it is found to be

$$\hat{\rho}_S(t) = \text{Tr}_B[\hat{\rho}(t)] = \sum_{\alpha, \beta} c_\alpha c_\beta^* e^{-i(E_\alpha - E_\beta)t} F_{\alpha\beta}(t) |E_\alpha\rangle \langle E_\beta|, \quad (\text{B3})$$

where c_α are complex coefficients in the system eigenbases $|E_\alpha\rangle$ with eigenenergies E_α . We have assumed that the combined system and bath are initialized in a product state $\hat{\rho}(0) = \hat{\rho}_S(0) \otimes \hat{\rho}_B(0)$, where $\hat{\rho}_S(0) = \sum_{\alpha, \beta} c_\alpha c_\beta^* |E_\alpha\rangle \langle E_\beta|$ and $\hat{\rho}_B(0)$

are the system and bath initial density matrices. In addition, we assume the two baths initially to be $\hat{\rho}_B(0) = \hat{\rho}_{\text{MB}}(0) \otimes \hat{\rho}_{\text{NMB}}(0)$, a product of thermal states with inverse temperatures β_{MB} and β_{NMB} , respectively. This means that $\hat{\rho}_a(0) = e^{-\beta_a \hat{H}_a} / Z_a$, where $Z_a = \text{Tr}[e^{-\beta_a \hat{H}_a}]$ with $a \in \{\text{MB}, \text{NMB}\}$. Moreover,

$$\begin{aligned} F_{\alpha\beta}(t) &= e^{-\gamma^0 t (V^{(\alpha)} - V^{(\beta)})^2} \text{Tr}[\hat{\rho}_{\text{NMB}}(0) e^{i\hat{H}_{SB}^{(\beta)} t} e^{-i\hat{H}_{SB}^{(\alpha)} t}] \\ &= e^{-\Gamma(t)(V^{(\alpha)} - V^{(\beta)})^2 + i\Lambda(t)([V^{(\alpha)}]^2 - [V^{(\beta)}]^2)} \end{aligned} \quad (\text{B4})$$

is the time-dependent influence functional that dictates the incoherent processes of the reduced system dynamics, with the functions

$$\Lambda(t) = \sum_l \left(\frac{g_l}{\omega_l} \right)^2 [\omega_l t - \sin(\omega_l t)], \quad (\text{B5})$$

$$\Gamma(t) = \gamma^0 t + \sum_l \left(\frac{g_l}{\omega_l} \right)^2 [1 - \cos(\omega_l t)] \coth \left(\frac{\beta_{\text{NMB}} \omega_l}{2} \right). \quad (\text{B6})$$

The dephasing rate γ^0 is due to the coupling to the Markovian bath. With the constraint Eq. (B2), \hat{H}_S and \hat{V}_S can be simultaneously diagonalized in the same bases, i.e., $\hat{V}_S |E_\alpha\rangle = V_S^{(\alpha)} |E_\alpha\rangle$, where $V_S^{(\alpha)}$ denotes the eigenvalue of the operator \hat{V}_S , and $|E_\alpha\rangle$ are eigenvectors of the Hamiltonian \hat{H}_S . The operator $\hat{H}_{SB}^{(\alpha)}$ appearing in Eq. (B4) reads $\hat{H}_{SB}^{(\alpha)} = V_S^{(\alpha)} \sum_l g_l (\hat{b}_l^\dagger + \hat{b}_l)$. We note that for each eigenstate $|E_\alpha\rangle$ the Hamiltonian $\hat{H}_{SB}^{(\alpha)}$ describes a set of displaced bosonic harmonic oscillators the displacement of which is proportional to the quantity $g_l V_S^{(\alpha)} / \omega_l$ [49].

When we take the time derivative of the exact solution for $\hat{\rho}_S(t)$ in Eq. (B3), we arrive at

$$\frac{d\hat{\rho}_S(t)}{dt} = \hat{\mathcal{L}}(t) \hat{\rho}_S(t) = -i[\hat{H}^S(t), \hat{\rho}_S(t)] + \gamma(t) \hat{\mathcal{D}}[\hat{V}_S] \hat{\rho}_S(t), \quad (\text{B7})$$

where the Lindblad superoperator is $\hat{\mathcal{D}}[\hat{V}_S] \hat{\rho}_S(t) = \hat{V}_S \hat{\rho}_S(t) - \frac{1}{2} (\hat{V}_S^2 \hat{\rho}_S(t) + \hat{\rho}_S(t) \hat{V}_S^2)$ and $\hat{H}^S(t) = \hat{H}^S - \lambda(t) \hat{V}_S^2$.

We have so far derived a time-local Lindblad master equation, Eq. (B7), with time-dependent rates $\gamma(t)$, composed of γ_0 (the Markovian contribution) and $\gamma_1(t)$. It is commonly accepted that when one of the dissipation rates $\gamma(t)$ becomes negative at a certain time interval the dynamics is referred to as non-Markovian [58–60]. In contrast, if the rates are positive at all times the evolution is considered Markovian. In the non-Markovian regime, there is back-flow of information between the system and environment [58–60]. This means that when the rates are positive the bath destroys coherent properties of the system. Contrary to this, when the rates are negative, the bath restores the lost information partially.

In order to involve the Floquet stroboscopic divisibility, we impose periodicity $\hat{\mathcal{L}}(t + T) = \hat{\mathcal{L}}(t)$ in the time-local master equation we obtain above, $\frac{d\hat{\rho}_S(t)}{dt} = \hat{\mathcal{L}}(t) \hat{\rho}_S(t)$, where $\hat{\mathcal{L}}$ is a time-periodic Liouvillian operator (LO). This is possible if we choose the frequencies of the non-Markovian bath to be $\omega_j = j\Omega$ with j being the integer multiples. The fundamental frequency Ω determines the period $T = 2\pi/\Omega$ of the Liouvillian. Therefore, all the interesting properties of the Floquet

theory can be directly applied [49]. For instance, one can define a propagator $\hat{\Phi}(t; 0)$, or dynamical map, such that $\hat{\rho}_S(t) = \hat{\Phi}(t; 0)\hat{\rho}_S(0)$. Due to the periodic nature of the LO, the dynamical map is divisible at stroboscopic times and we have $\hat{\Phi}(mT; 0) = [\hat{\Phi}(T; 0)]^m$. Thus, one can focus the system dynamics just for one time period, due to the periodic nature of the master equation. Furthermore, we assume that the non-Markovian bath is prepared initially at near-zero temperature, i.e., $\beta_{NM} \rightarrow \infty$, and consider couplings $g_j = (\eta/\Omega^2)e^{-zj/2}$,

where $z > 0$ is a positive number. In this way, one can couple an arbitrary quantum system with both Markovian and non-Markovian environments. Furthermore, one is able to tune the system-bath couplings explicitly, which is useful for quantum bath engineering. In the main text, we have corroborated the general idea developed here with a standard example of a quantum Ising spin chain in a periodic boundary condition, and look for the DQPT signatures via the fidelity Loschmidt amplitude.

-
- [1] S. Sachdev, *Quantum Phase Transitions* (Cambridge University Press, Cambridge, 2011).
 - [2] S. Suzuki, J.-I. Inoue, and B. K. Chakrabarti, *Quantum Ising Phases and Transitions in Transverse Ising Models*, Lecture Notes in Physics (Springer, New York, 2012), Vol. 862.
 - [3] C.-N. Yang and T.-D. Lee, *Phys. Rev.* **87**, 404 (1952).
 - [4] T.-D. Lee and C.-N. Yang, *Phys. Rev.* **87**, 410 (1952).
 - [5] M. E. Fisher, *Lectures in Theoretical Physics. Vol. 7C: Statistical Physics, Weak Interactions, Field Theory: Lectures Delivered at the Summer Institute for Theoretical Physics, University of Colorado, Boulder, 1964* (University of Colorado Press, Boulder, 1965).
 - [6] F. Pollmann, S. Mukerjee, A. G. Green, and J. E. Moore, *Phys. Rev. E* **81**, 020101(R) (2010).
 - [7] M. Heyl, A. Polkovnikov, and S. Kehrein, *Phys. Rev. Lett.* **110**, 135704 (2013).
 - [8] B. Žunkovič, M. Heyl, M. Knap, and A. Silva, *Phys. Rev. Lett.* **120**, 130601 (2018).
 - [9] J. C. Halimeh and V. Zauner-Stauber, *Phys. Rev. B* **96**, 134427 (2017).
 - [10] V. Zauner-Stauber and J. C. Halimeh, *Phys. Rev. E* **96**, 062118 (2017).
 - [11] I. Homrighausen, N. O. Abeling, V. Zauner-Stauber, and J. C. Halimeh, *Phys. Rev. B* **96**, 104436 (2017).
 - [12] J. Lang, B. Frank, and J. C. Halimeh, *Phys. Rev. B* **97**, 174401 (2018).
 - [13] J. C. Halimeh, M. Van Damme, V. Zauner-Stauber, and L. Vanderstraeten, arXiv:1810.07187 (2018).
 - [14] M. Moeckel and S. Kehrein, *Phys. Rev. Lett.* **100**, 175702 (2008).
 - [15] M. Moeckel and S. Kehrein, *New J. Phys.* **12**, 055016 (2010).
 - [16] B. Sciolla and G. Biroli, *Phys. Rev. Lett.* **105**, 220401 (2010).
 - [17] B. Sciolla and G. Biroli, *J. Stat. Mech.* (2011) P11003.
 - [18] A. Gambassi and P. Calabrese, *Europhys. Lett.* **95**, 66007 (2011).
 - [19] B. Sciolla and G. Biroli, *Phys. Rev. B* **88**, 201110(R) (2013).
 - [20] A. Maraga, A. Chiocchetta, A. Mitra, and A. Gambassi, *Phys. Rev. E* **92**, 042151 (2015).
 - [21] T. Mori, T. N. Ikeda, E. Kaminishi, and M. Ueda, *J. Phys. B* **51**, 112001 (2018).
 - [22] J. Zhang, G. Pagano, P. W. Hess, A. Kyprianidis, P. Becker, H. Kaplan, A. V. Gorshkov, Z.-X. Gong, and C. Monroe, *Nature (London)* **551**, 601 (2017).
 - [23] J. C. Halimeh, V. Zauner-Stauber, I. P. McCulloch, I. de Vega, U. Schollwöck, and M. Kastner, *Phys. Rev. B* **95**, 024302 (2017).
 - [24] C. Karrasch and D. Schuricht, *Phys. Rev. B* **87**, 195104 (2013).
 - [25] F. Andraschko and J. Sirker, *Phys. Rev. B* **89**, 125120 (2014).
 - [26] M. Heyl, *Phys. Rev. Lett.* **113**, 205701 (2014).
 - [27] P. Jurcevic, H. Shen, P. Hauke, C. Maier, T. Brydges, C. Hempel, B. P. Lanyon, M. Heyl, R. Blatt, and C. F. Roos, *Phys. Rev. Lett.* **119**, 080501 (2017).
 - [28] M. Heyl, *Rep. Prog. Phys.* **81**, 054001 (2018).
 - [29] L. Piroli, B. Pozsgay, and E. Vernier, *Nucl. Phys. B* **933**, 454 (2018).
 - [30] J. Lang, B. Frank, and J. C. Halimeh, *Phys. Rev. Lett.* **121**, 130603 (2018).
 - [31] H. T. Quan, Z. Song, X. F. Liu, P. Zanardi, and C. P. Sun, *Phys. Rev. Lett.* **96**, 140604 (2006).
 - [32] Y.-C. Li and S.-S. Li, *Phys. Rev. A* **76**, 032117 (2007).
 - [33] B.-B. Wei and R.-B. Liu, *Phys. Rev. Lett.* **109**, 185701 (2012).
 - [34] B. Dóra, F. Pollmann, J. Fortágh, and G. Zaránd, *Phys. Rev. Lett.* **111**, 046402 (2013).
 - [35] B.-B. Wei, S.-W. Chen, H.-C. Po, and R.-B. Liu, *Sci. Rep.* **4**, 5202 (2014).
 - [36] S. Suzuki, T. Nag, and A. Dutta, *Phys. Rev. A* **93**, 012112 (2016).
 - [37] K. Choo, U. Bissbort, and D. Poletti, *Eur. Phys. J.: Spec. Top.* **227**, 313 (2018).
 - [38] A. A. Zvyagin, *Low Temp. Phys.* **42**, 971 (2016).
 - [39] M. Heyl and J. C. Budich, *Phys. Rev. B* **96**, 180304(R) (2017).
 - [40] N. Fläschner, D. Vogel, M. Tarnowski, B. S. Rem, D.-S. Lühmann, M. Heyl, J. C. Budich, L. Mathey, K. Sengstock, and C. Weitenberg, *Nat. Phys.* **14**, 265 (2018).
 - [41] X.-Y. Guo, C. Yang, Y. Zeng, Y. Peng, H.-K. Li, H. Deng, Y.-R. Jin, S. Chen, D. Zheng, and H. Fan, *Phys. Rev. Appl.* **11**, 044080 (2019).
 - [42] S. Vajna and B. Dóra, *Phys. Rev. B* **91**, 155127 (2015).
 - [43] D. Trapin and M. Heyl, *Phys. Rev. B* **97**, 174303 (2018).
 - [44] U. Bhattacharya, S. Bandyopadhyay, and A. Dutta, *Phys. Rev. B* **96**, 180303(R) (2017).
 - [45] N. Sedlmayr, M. Fleischhauer, and J. Sirker, *Phys. Rev. B* **97**, 045147 (2018).
 - [46] B. Mera, C. Vlachou, N. Paunković, V. R. Vieira, and O. Viyuela, *Phys. Rev. B* **97**, 094110 (2018).
 - [47] S. Bandyopadhyay, S. Laha, U. Bhattacharya, and A. Dutta, *Sci. Rep.* **8**, 11921 (2018).
 - [48] H. Lang, Y. Chen, Q. Hong, and H. Fan, *Phys. Rev. B* **98**, 134310 (2018).
 - [49] V. M. Bastidas, T. H. Kyaw, J. Tangpanitanon, G. Romero, L.-C. Kwek, and D. G. Angelakis, *New J. Phys.* **20**, 093004 (2018).

- [50] T. Antal, Z. Rácz, and L. Sasvári, *Phys. Rev. Lett.* **78**, 167 (1997).
- [51] L.-A. Wu and D. Segal, *J. Phys. A* **42**, 025302 (2008).
- [52] I. Dzyaloshinsky, *J. Phys. Chem. Solids* **4**, 241 (1958).
- [53] T. Moriya, *Phys. Rev.* **120**, 91 (1960).
- [54] C. Addis, B. Bylicka, D. Chruściński, and S. Maniscalco, *Phys. Rev. A* **90**, 052103 (2014).
- [55] A. Rivas, S. F. Huelga, and M. B. Plenio, *Phys. Rev. Lett.* **105**, 050403 (2010).
- [56] H.-P. Breuer, E.-M. Laine, and J. Piilo, *Phys. Rev. Lett.* **103**, 210401 (2009).
- [57] S. Luo, S. Fu, and H. Song, *Phys. Rev. A* **86**, 044101 (2012).
- [58] A. Rivas, S. F. Huelga, and M. B. Plenio, *Rep. Prog. Phys.* **77**, 094001 (2014).
- [59] H.-P. Breuer, E.-M. Laine, J. Piilo, and B. Vacchini, *Rev. Mod. Phys.* **88**, 021002 (2016).
- [60] I. de Vega and D. Alonso, *Rev. Mod. Phys.* **89**, 015001 (2017).